Flowslide Due to Liquefaction in Petobo during the 2018 Palu Earthquake

Mahdi Ibrahim Tanjung[1], Masyhur Irsyam[1], Andhika Sahadewa[1], Susumu Iai[2], Tetsu-oTobita[3], and Hasbullah Nawir[1]

[1] Bandung Institute of Technology, Bandung, Indonesia
[2] Kyoto University, Kyoto, Japan
[3] Kansai University, Osaka, Japan
sahadewa@itb.ac.id

Abstract.
The 2018 Palu Earthquake in Indonesia triggered liquefaction that was followed by many incidents, including in massive flowsides in Petobo. In this location, flowsides with deformations reaching 1 km occurred on gentle slopes. The liquefaction mechanism causing this enormous lateral deformation is not fully understood yet. In fact, a comprehensive understanding of this phenomenon mechanism can be used to mitigate similar disasters in the future. This study describes the flow slide observations in Petobo based on geotechnical investigations, including trench, geophysical survey, CPT, boreholes, and laboratory testing. The investigation showed that the flow slide location consisted of alternating layers with high and low permeabilities. The high permeability difference during pore water pressure dissipation in the liquefied layer resulted in void redistribution in layers overlain by low permeability layer. This void ratio increase triggered a significant shear strength loss in the corresponding layer. This study also shows that differences in the soil condition and the water table depth play important roles whether a location experiences a flow slide or not. The results of this study are expected to enrich our knowledge related to liquefaction induced flow slide and can be used as a basis to evaluate flow slide potential in other locations.

Keywords: Flowslide, Liquefaction, void redistribution, insitu test.

1 Introduction

An earthquake with moment magnitude (M_w) of 7.5 at depth of 10 km occurred in Palu, Central Sulawesi, Indonesia on September 28, 2018. The earthquake triggered large-scale liquefaction and flow slides in many areas in Palu. Baloroa, Petobo, Jono Oge, and Sibalaya are locations experienced the most disastrous flow slides (Sahadewa et al. 2019). Petobo and Balaroa are mostly residential areas, while Jono Oge and Sibalaya are dominated by agricultural lands. These four areas are located 80 – 110 km from the epicenter. The earthquake acceleration recorded on the surface near Balaroa, identified as a SC site class, showed peak earthquake acceleration values of 0.207 g (NS), 0.286 g (EW), and 0.341 g (UD) as reported by Okamura (2019). Amongst the four areas, Petobo experienced the largest loss of life as well as the largest flow side area of 1.43

km^2 (Mason, 2019). This area was a gentle slope with a shallow soil thickness prior to the earthquake.

Geographically, these 4 locations are similar, where flow slide locations were located at the end of the alluvial river descending from the hill to the valley of Palu city (Okamura, 2019; Mason, 2019). Most of river alluvial is sandy gravel. In the location of flow slide foot, finer materials, such as clay and silt were observed between sand and gravel layers (JICA, 2019). Topographically, these 4 locations are basin where the groundwater level is shallow. In the east side of the flow slide locations, except in Balaroa, the groundwater level near the flow slide crown was also affected by the Gumbasa irrigation channel, although each location has different groundwater level characteristics.

Flow slide event due to liquefaction as large as those of Palu is very rare. The true mechanism is not clearly understood and has been an attractive subject for discussion. Several possible mechanisms include the formation of a water film due to redistribution of voids (Kokusho, 1999), shear failure due to seepage (Sento, 2004), the effect of non-cohesive content on the liquefied material that leads this material to contractive deformation (Okamura, 2019), and another mechanism is void redistributions resulting in void ratio increases in more impermeable layers that lead to significant shear strength reduction. This paper presents summary of the latest results of field investigations in Petobo and the associated laboratory tests as an effort to understand the flow slide mechanism.

2 Ground movements

Aerial photos of Petobo before and after the 2018 Palu Earthquake were used to analyze the flow slides. A total of 49 scattered objects in the flow slide area, including houses, channels, and trees, was traced to identify the direction and magnitude of the ground surface displacement. The displacement vectors on the topography contour post-earthquake are presented in **Fig. 1**. The flow slide length from the crown to the toe is 2150 m. In general, the flow slide moved from the east to the west in the direction perpendicular to the contour lines.

The largest flow slide displacement is around 1000 m in the east-central part, as shown as red line in **Fig. 1**, about 250 m from the irrigation channel. In general, the displacement magnitude increased from the crown to the point with the greatest displacement, whereas the displacement decreased from this point to landslide foot. Petobo's deformation pattern is similar to other locations that have smaller displacements, such as one in between Petobo and Jono Oge (Bradley, 2019). **Fig. 2** shows the relationship between displacement (d) and distance to the landslide crown (s) in Petobo. This figure shows that the relationship at s values ranging from 250 m to the flow slide foot is linear. this shows that the strain occurring in the compressed crust is relatively the same throughout the compression area. The strain magnitude is probably influenced by the thickness of the flow slide crust. Additionally, the point experiencing the largest movement was predicted as the initial position of the flow slide, which was followed by landslides moving to the irrigation channel.

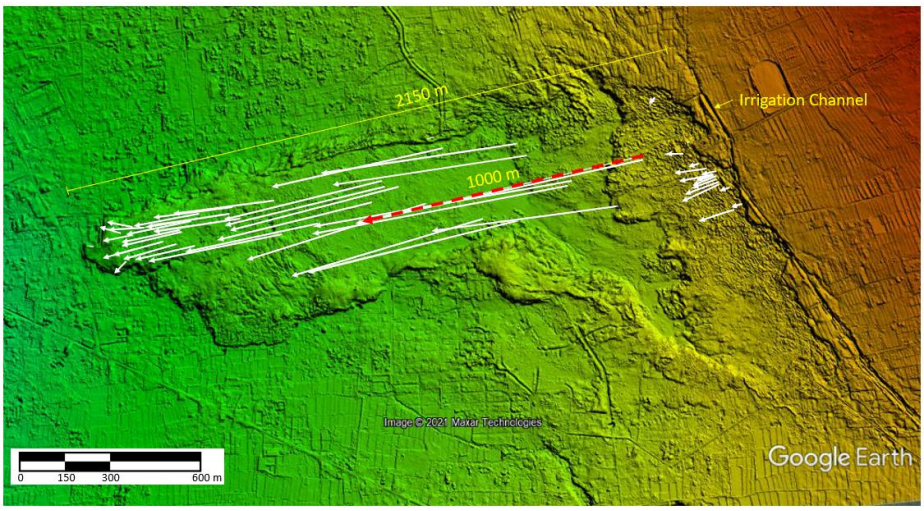

Fig. 1. Displacement vectors and contours after flowslide

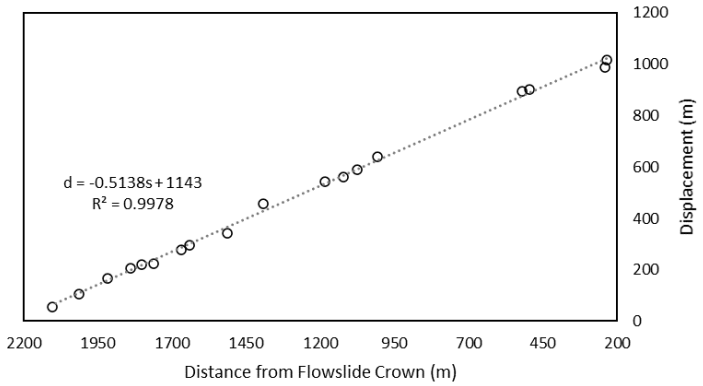

Fig. 2. Variation of displacement with distance to crown flowslide

3 Identification of liquefied layer

Soil profile and groundwater table depth are keys to understand landslide mechanism due to liquefaction. Therefore, 2 trenches were excavated on the east side of flow slide area in Petobo. On the trench wall, several samples were taken for laboratory testing, particularly in the layers that were considered liquefied and the impermeable layers which became the capping layers. A series of Multi-channel Analysis of Surface Wave (MASW) tests was performed nearby the trenches to evaluate the variation of shear wave velocity (V_S) with depth. In addition, secondary data from previous field investigations was collected, including 7 borehole points by JICA (2019) (**Fig. 5**) and 9 Cone

Penetration Test (CPT) points by PT. Promisco (**Fig. 6** and **Fig. 7**). The location of all geotechnical investigations in Petobo presented in **Fig. 3**.

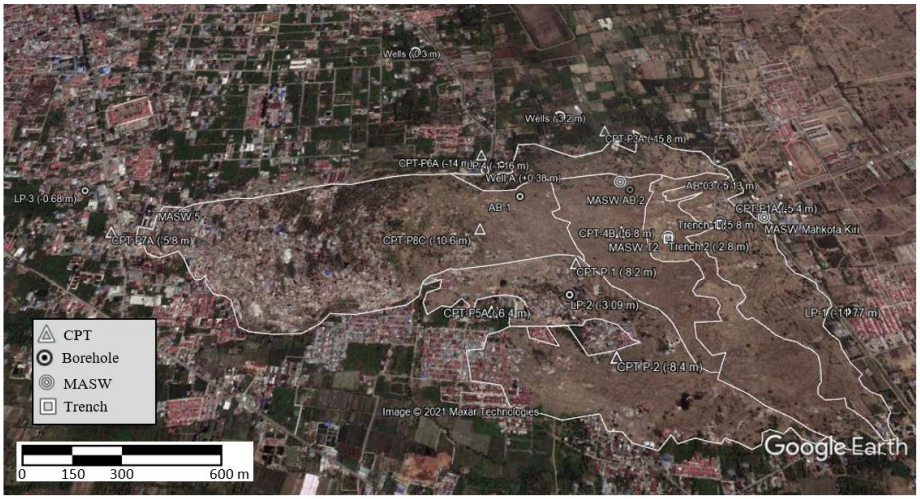

Fig. 3. Map of the distribution of geotechnical investigation in Petobo

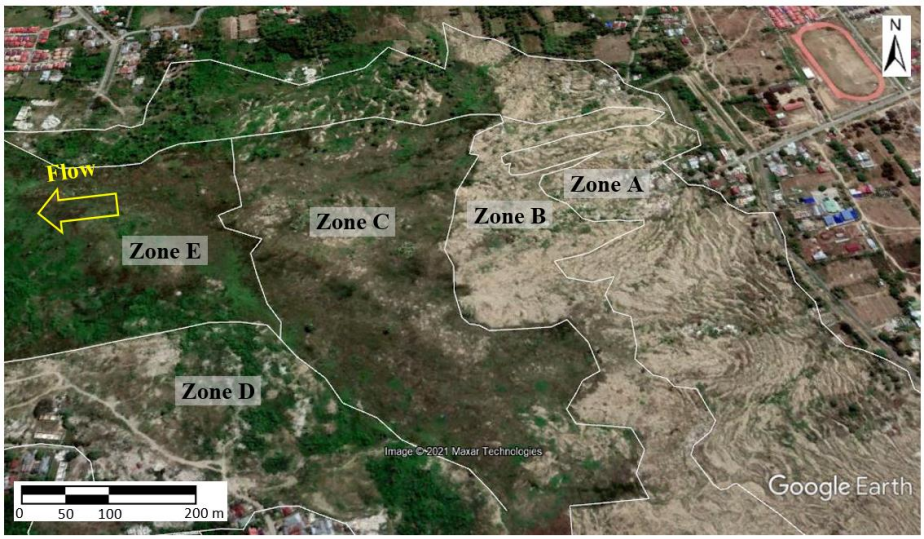

Fig. 4. Flowslide zone based on morphological features

The flow slide area generally can be divided into 5 zones based on the morphological appearance post-earthquake (**Fig. 4**). Zone A is an area that experienced widening and overturning. Zone B is an area that liquefaction was more pronounce resulting flatter morphology with only few soil blocks left intact. Zone C is the foundation that became the slip plane whose surface was then partially overlain by Zone B. Zone D is an area

consisting of deposited materials to the south of flow slide which was highly liquefied post-earthquake. Zone E has similar deposited material to Zone D. But Zone E experienced a much larger runout distance than Zone D. Zone C and Zone E were very wet. Water started to seep at the boundary between Zone B and zone C. Subsequently, the water accumulated in Zone E which has very flat terrain.

Field investigation results were studied to evaluate the soil profile in each zone. Soil layer in Zone A was characterized using Trench 1 and borehole AB-3. Layering in Zone B was evaluated using Trench 2. Soil profile in Zone C was assessed using bore hole AB-2 and CPT 4B. Subsurface condition in Zone D was identified using CPT P1. Meanwhile, soil layer in Zone E was evaluated using the borehole AB-1 and CPT P8C. Soil profile identifications were also performed in the flow slide boundary area. The toe area was evaluated using CPT P7A. The crown area was characterized using CPT-P1A. The left side of the flow slide was evaluated using points CPT P-1, CPT P-2, and CPT P5A. The right side of the flow slide was identified by points CPT P6A.

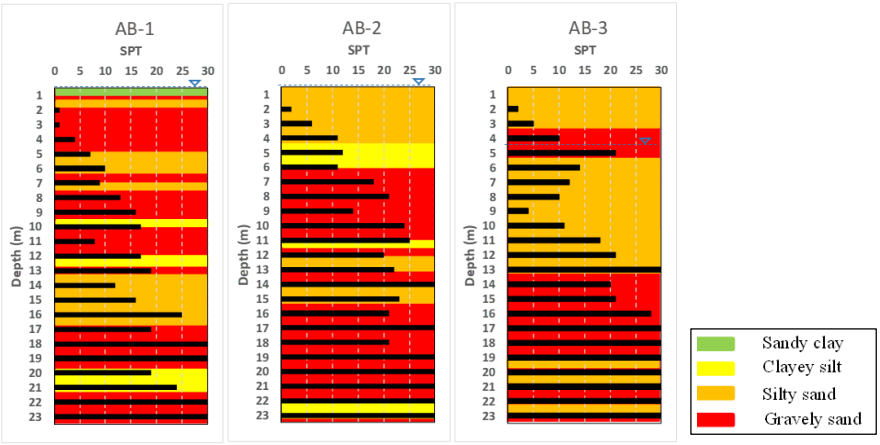

Fig. 5. Soil layer profile and SPT in the middle of the flow slide (JICA, 2019)

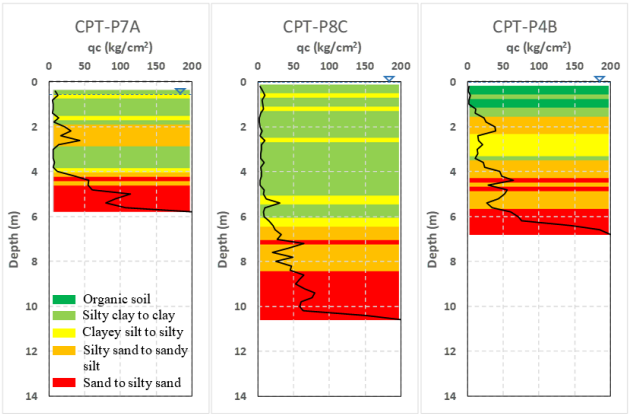

Fig. 6. Soil layer profile and cone resistance in the middle of the flowslide area

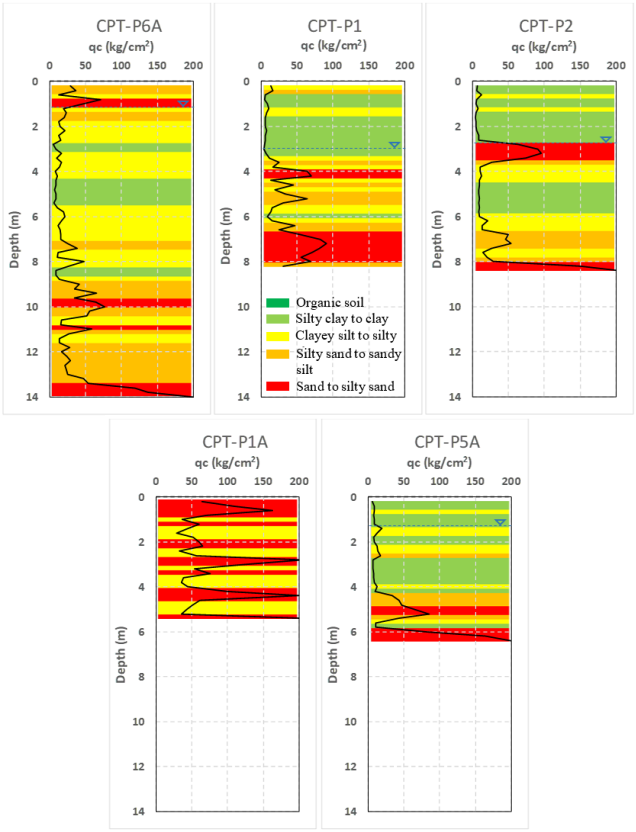

Fig. 7. Soil layer profile and cone resistance on the outside of the flowslide area

Trench 1, in Zone A, was excavated to depth of 7 m. The ground water table was found at depth of 5.85 m. This observation was relatively consistent with ground water table found at depth of 5.13 m in borehole AB-3. The layer profile in Trench 1 alternated between coarse grained materials (i.e., sand and gravelly sand) with sandy silt or silty clay (**Fig. 8**). This pattern was similar to that of boreholes and CPT results. In Trench 1, a relatively impermeable layer of silty clayey sand was observed at depth of 3.85 m – 5.85 m interspersed with a thin layer of sand. The thin sand layer was found not continuous. This segregation may be attributed to layer stretching during flow slide.

All layers in Trench 1 had relatively low V_s values, which were less than 230 m/s. The lowest V_s value of 143 m/s was observed in the gravely sand layer containing sandy silt. The silty clay layer with alternating thin sand layers had a slightly higher V_s value of 162 m/s. This low V_s in gravely sand layer may indicate that this layer has experienced liquefaction. The gravely sand layer found at depth of 5.85 m or greater, below the silty clayey sand layer, had a V_s of 204 m/s and was prone to liquefaction. The silty clayey sand layer above it was suspected as a capping layer. At depth of 7 m – 8.9 m

and greater, the V_s value increased with depth (**Fig. 10**). These layers were more resistant to liquefaction with the lowest V_s value of 248 m/s.

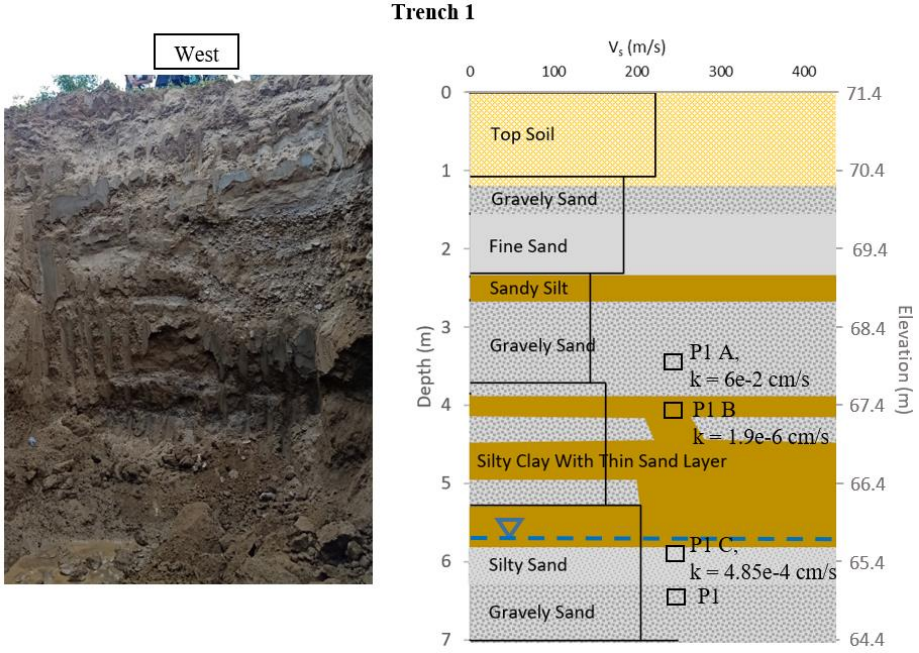

Fig. 8. Stratification of soil layer on the wall of trench 1

Trench 2, located in Zone B, was excavated to depth of 3 m (**Fig. 9**). The ground water level was encountered at depth of 2.85 m. The layer profile in Trench 2 wall was relatively similar to that of Trench 1. In this case, alternating sand or gravely sand with a more impermeable layer of sandy silt was observed (**Fig. 9**). In Trench 2, there was no impermeable layer as thick as in Trench 1. The thickness of the impermeable layer in Trench 2 was only around 15 cm – 35 cm. The V_s values in Trench 2 were very small, ranging from 123 m/s – 154 m/s. Due to this fact, the layer in Trench 2 wall was suspected to experience liquefaction during earthquake. Layers having quite high V_s (> 300 m/s) and small liquefaction potential were observed at depth of 5.27 m or deeper (**Fig. 10**).

A cross-section showing the flow slide that passed through the trench test site and nearby field investigations are presented in **Fig. 11**. Liquefaction potential is identified as the yellow layer. The green layer shows more impermeable layer. The black dotted line indicates the possible slip plane occurring along the flow slide. Above this line, materials slid to the slope foot, while materials below the line remained in place.

Based on Petobo terrain, the flow slide occurred in an area with slope of 0.5° – 2.2°. Flow slide flew quite far in an area with slope of $\pm 0.5^\circ$, forming a nearly flat area on the flow slide surface. The flow slide area in Petobo has a groundwater depth of less than 4 m.

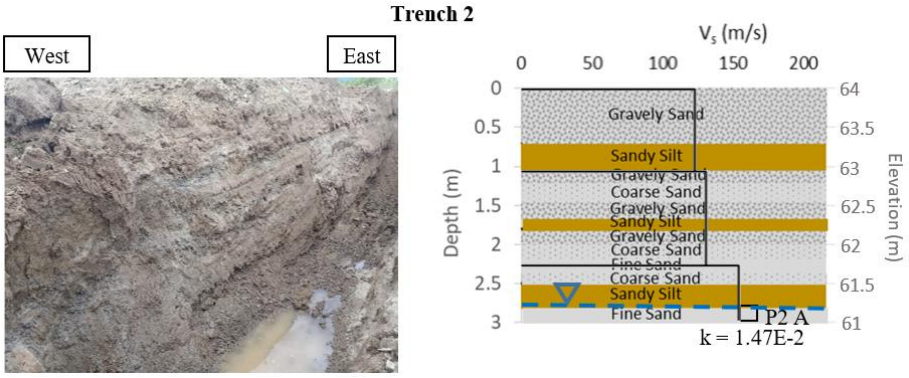

Fig. 9. Stratification of soil layer on the wall of trench 2

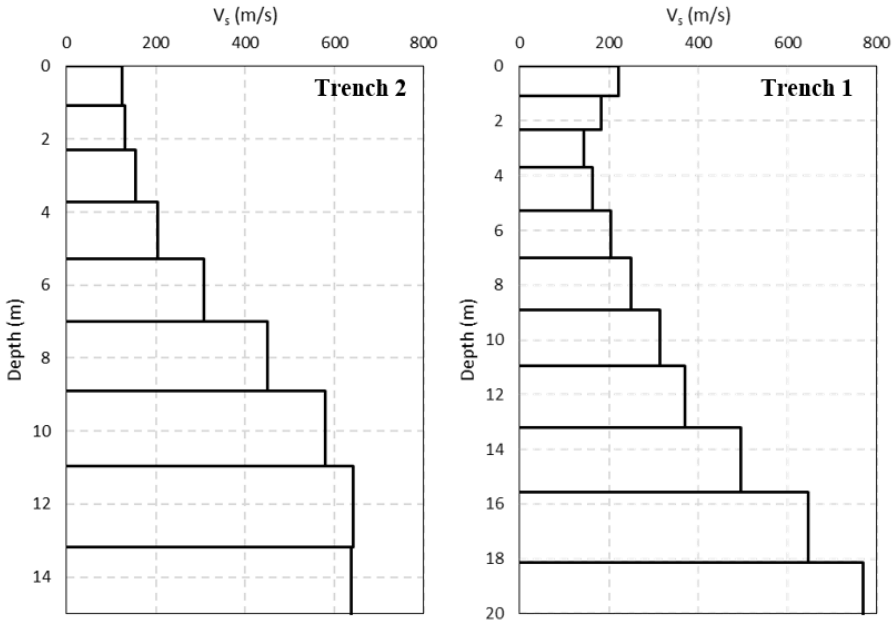

Fig. 10. Shear wave velocity profile in trench 1 and trench 2

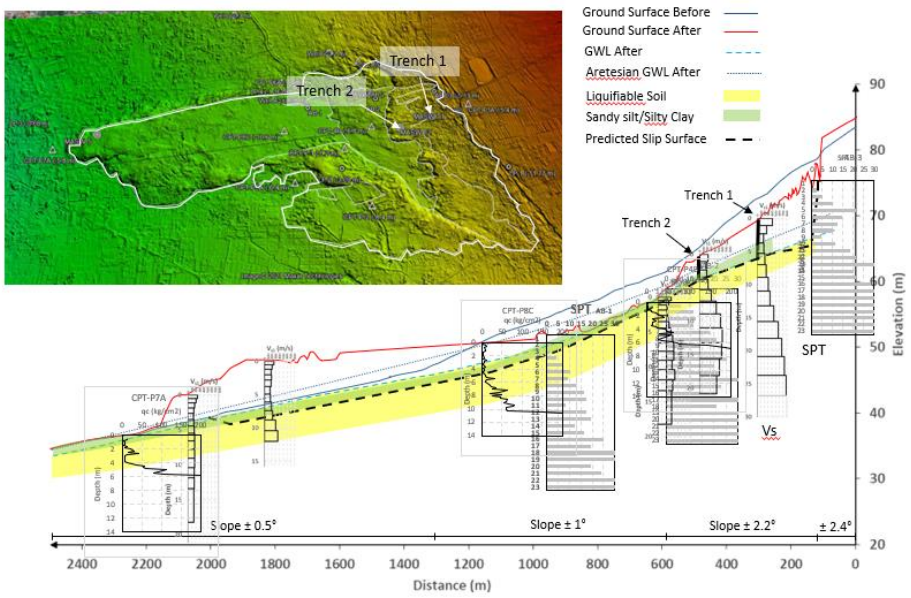

Fig. 11. Geotechnical Investigation Compilation in Petobo

4 Laboratory test

A series of laboratory testing was performed on samples obtained from the trench walls, including grain size distribution, Atterberg limits, and permeability tests (**Fig. 12** and **Table 1**). Cyclic and monotonic direct simple shear tests were conducted on samples collected from layers where liquefaction was expected. These direct shear tests allow us to assess the soil response due to cyclic loading and the effect of volume changes on residual shear strength (**Fig. 13**). Additionally, a liquefaction test using tubes was carried out to evaluate void redistribution process and water pressure dissipation (**错误!未找到引用源。**). Furthermore, ejecta sand materials on the surface were also collected.

Trench soil profile and the corresponding lab results are shown in **Fig. 8**, **Fig. 9**, and **Table 1, respectively.** The gradation test showed samples from the trench wall containing fine sand and gravely sand with fine content less than 20%. It is different from the ejecta sand that was consisted of more than 20% fine grain content. This difference may be attributed to suffusion, a phenomenon where fine particle migration occurs due to seepage flow through pre-existing pores in coarse particle. In this case, during pore water pressure dissipation process, clay or silt contents were carried out upward by water flow across the voids of coarse grain soils. Field observation showed that the sand columns, where the ejecta sand escaped, consisted of coarser grains than that of materials accumulated on the surface. During pore water pressure dissipation, it appears that suffusion process was also accompanied by segregation occurred when liquefied sand

material flew to the surface. This event was also observed in liquefaction tube test, where the fine grains accumulated above the liquefied layer.

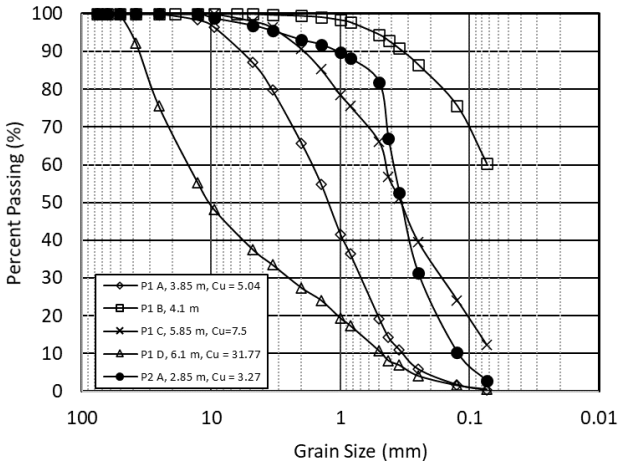

Fig. 12. Soil grain size distribution obtained from trench

Table 1. Laboratory test result obtained from trench

Parameter	P1 A	P1 B	P1 C	P1 D	P2 A
Gravel (%)	12.95	-	5.59	62.43	3.08
Sand (%)	86.68	39.76	86.79	36.98	94.18
#200 (%)	0.37	60.24	7.62	0.59	2.74
Cu	5.04	-	7.5	31.769	3.266
Cc	0.861	-	1	1.047	1.191
LL (%)	-	27.25	-	-	-
PI (%)	-	9.5	-	-	-
USCS	SP	CL	SW	GW	SP
k (cm/s)	$6.04x10^{-2}$	$1.9x10^{-6}$	$4.85x10^{-4}$	-	$1.47x10^{-2}$

The impermeable layer above the coarse grain layer contained more than 60% fines **Fig. 8**. Seed (2003) suggests that this layer are prone to liquefaction based on the IP and LL values. Thus, in addition to serving as a capping layer due to low permeability, this layer can also serve as a slip plane.

The results of cyclic and monotonic direct simple shear tests indicate that the associated soil layer maybe liquefied during the 2018 Palu Earthquake (**Fig. 13**). The monotonic test showed that a layer may experience void redistribution due to temporary retention of the volume of water dissipated from the liquefied layer below it. This void redistribution leads to an increase in volume that results in decreases in effective stress and shear strength in large strains.

The liquefaction tube test facilitates observation of the distributions of sand grain movement and pore water pressure during dissipation. This test was performed by putting liquefiable soil layer in a transparent acrylic tube. Above this layer, a cap layer having lower permeability was placed. Three pore water pressure gauges were installed

at 16 cm, 40 cm, and 60 cm from the bottom of the tube. A rubber mallet was used to hit the tube generating vibration. A high-resolution camcorder was used to record the event.

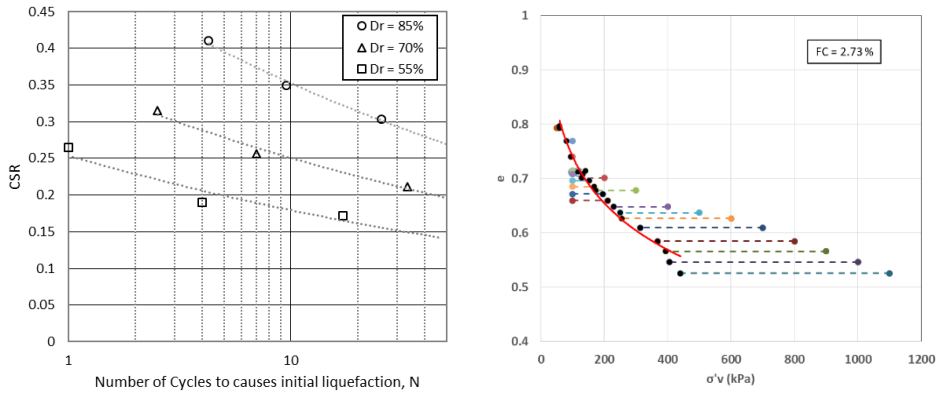

Fig. 13. Cyclic and monotonic test results from sample P2A

Soil profile post liquefaction tube test after is shown in **错误!未找到引用源。** (a). A water film, indicated by blue line in **错误!未找到引用源。** (a), appeared when the liquefied soil layer settled due to excess pore water pressure dissipation. The thickness of this water film increases with the magnitude of liquefaction-induced settlement. Soil settlement due to excess pore water pressure dissipation is proportional to the extent of excess pore water pressure generated during dynamic loading. Excess pore water pressure depends on the relative density of the soil. The denser the soil layer, the smaller the generated excess pore water pressure is. The smaller the generated pore water pressure, the smaller the liquefaction settlement layer is. Thus, the denser the soil, the thinner the formed water film is.

The water film was formed for some time until the pore water pressure below the cap layer was dissipated. The duration of water film occurrence depended on the permeabilities of the cap layer and the liquefied soil. The pore water pressure dissipation process length at each depth of the liquefied layer was proportional to the increase in the pore water pressure. Thus, the slope of the pore water pressure versus depth during the dissipation process was equal to that of pre-liquefaction occurrence (**错误!未找到引用源。** (c)). The dissipation process was affected by the cap layer. The excess pore water pressure could not be directly dissipated to the initial pore water pressure. In fact, no reduction in pore water pressure was observed for a while until it dissipated through the cap layer. If the cap layer is very impermeable or very thick, the excess pore water pressure will be trapped longer.

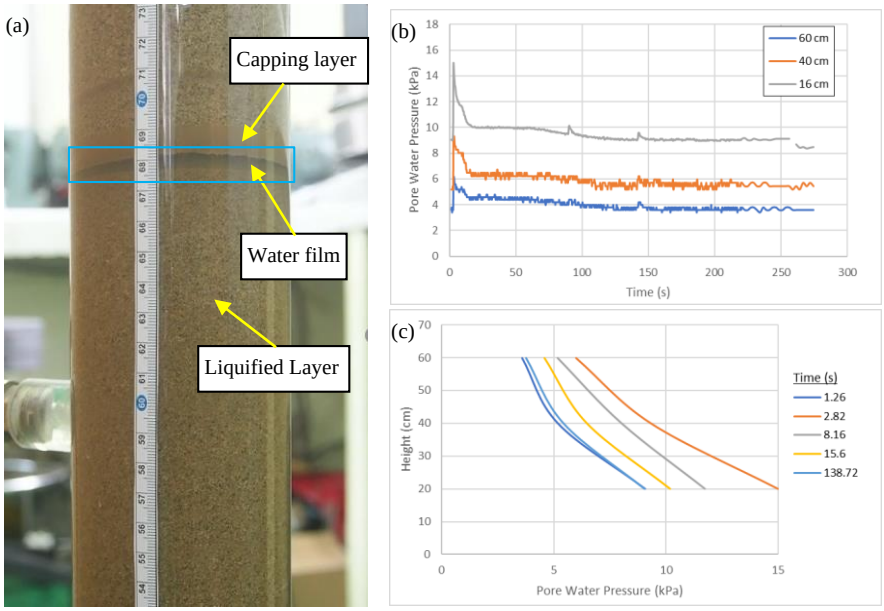

Fig. 14. (a) Post Liquefaction Tube Test, (b) Variation of Pore Water Pressure Dissipation with Time, and (c) Variation of Pore Water Pressure with Depth

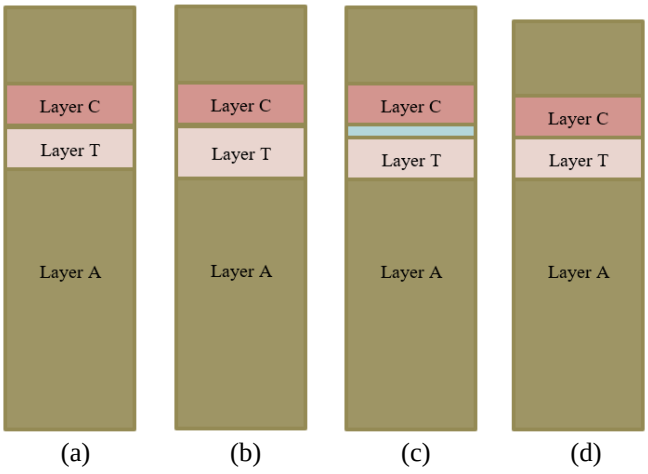

Fig. 15. Schematic of the water film formation process ((a) initial conditions, (b) pore water pressure dissipation process before the water film is formed, (c) pore water pressure dissipation process when the water film is formed, (d) finished pore water pressure dissipation

The liquefaction tube test showed that there was thin layer of about 2.5 cm (Layer T) before the water film was formed (**Fig. 15**). Immediately after liquefaction, Layer T did not settle, whereas Layer A did. Layer T started to settle with the forming of water film layer. This is probably because the pore water pressure released by Layer A is

trapped first in Layer T as it is blocked by Cap Layer (Layer C). When settlement in Layer A was overly large to be accommodated by the expansion of Layer T, ±0.5-cm water film was formed above Layer T. When the water film has formed, the pore water pressure trapped in the Layer T was then dissipated into the water film. When the pore water pressure was trapped in Layer T, this layer may experience significant strength reduction due to an increase in volume. After the water film was fully formed, the dissipation of pore water pressure below Layer C was visually identified by settlements of Layer C and layers above it. Subsequently, the pore water pressure returned to its initial pressure with the closure of water film.

Observation of strength degradation in Layer T suggested that the occurrence of this layer in the field, such as in Petobo, may trigger a flow slide due to liquefaction. Thus, in addition to the water film, the thin layer also contributed to the flow slide. It is also expected, even before the water film was formed, the slope has started to slip in this thin layer.

5 Flowslide reconstruction

Petobo flow slide generally can be divided into 2 liquefied blocks based on the deformation pattern (**Fig. 16**). The first block, colored brown, was the fluidized block. The second block, shown in orange, was part experiencing lateral extension and back rotation. Visual observation showed that the brown block was very liquidized with a maximum displacement of up to 1 km. This block initiated displacement that eventually triggered instability of the orange block. The orange block was not as liquid as the brown block and only displaced less than 130 m. This block apparently moved as an extended solid soil block with overturning near the landslide crown.

These orange and brown blocks contained potential liquefaction layers alternating with impermeable layers. The differences in displacement behavior between these blocks may be associated to the liquefied layer thickness and the crust layer thickness above the liquefied layer. The crust layer thickness is not only influenced by the type of soil layer but also greatly influenced by the depth of the water table. The water level in the brown block was less than 4 m, whereas that of orange block was deeper than 4 m. The liquefied layer thickness of the brown block was more than 2 m, while that of orange block was less than 2 m.

The slip plane was indicated occurring in an impermeable layer that served as a capping during liquefaction. Geotechnical investigation showed that mixtures of flow slide material were found above the liquefied layer in the brown block. Thus, the intact capping layer was difficult to identify. In the orange block, the impermeable layer that functions as capping was still intact along with the soil layer above it. The movement of the orange block did not damage the capping layer. With the movement pattern of these blocks, the liquefied soil layers did not experience much breakdown and were still under these blocks.

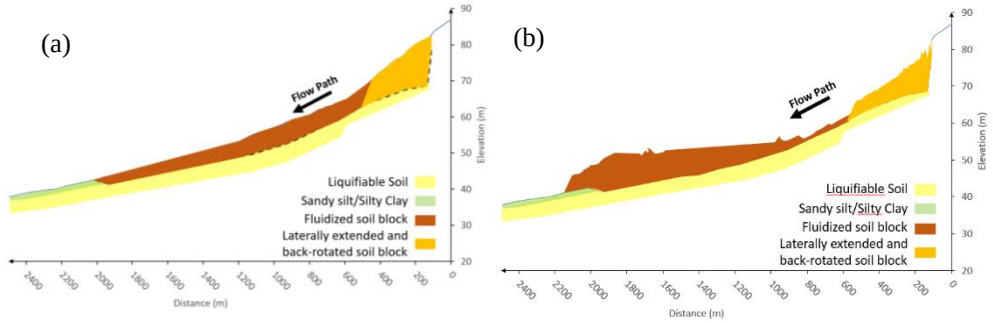

Fig. 16. Petobo flowslide schematization ((a) Before (b). After)

Kokusho (1999, 2003) described the flow slide as large soil deformation attributed to the formation of a water interlayer. In this hypothesis, a layer of water with almost zero shear strength is formed just above the liquefied layer immediately after the ground shaking. This layer is formed because the water pressure that is going to be dissipated into the layer above is covered by a more impermeable layer above it.

The flow slide mechanism cannot be comprehensively explained only based on the water film hypothesis (Okamura 2019). Liquefied nature of the soil itself is also attributed to flow slide. If the sand is very contractile and shows shear strength loss, it can experience very large strains. Kokusho (2015) stated that clean sand always shows a dilative response and there is small chance of a flow slide based on undrained shear test results.

Redistribution of voids is also another phenomenon associated with flow slide due to liquefaction. Void redistribution is an important factor affecting the residual shear strength after liquefaction and is greatly affected by the permeability. Void ratio increase can occur in layers that have lower permeability. This increase eventually leads to shear strength loss of the layer. The void redistribution scheme in confined sand layers on an infinite slope is described by Malvick (2006), Montgometry (2014), and Iai (2020).

6 Summary

An investigation of flow slide due to the 2018 Palu Earthquake in Petobo has been carried out and described in this paper. Petobo flow slide occurred in the shallow ground water table which subsequently drew the zone behind it that had deeper water elevation. The investigation showed that flow side area has layer of gravelly sand alternating with a more impermeable layers consisting of clay and silt. The liquefaction tube test showed that, after liquefaction triggering excess pore water pressure, the impermeable layer overlying the liquefied soil impeded the excess pore water pressure dissipation. In addition, during the dissipation process, the forming of a layer with increase in void ratio was observed. This void ratio increased with pore water pressure dissipation through the more impermeable layer. Layer experiencing void ratio increase was predicted to

trigger instability. The results of this investigation are expected to strengthen our understanding related to flow slide due to liquefaction and can mitigate flow slide potential in other locations.

References

1. Bradley, K., Mallick, R., Andikagumi, H., Hubbard, J., Meilianda, E., Switzer, A., Du, N., Brocard, G., Alfian, D., Benazir, B., et al..: Earthquake-triggered 2018 Palu valley landslides enabled by wet rice cultivation. Nat. Geosci. 12 (11), 935–939 (2019).
2. Iai S.: Paths Forward for Evaluating Seismic Performance of Geotechnical Structures. In: Kutter B., Manzari M., Zeghal M. (eds) Model Tests and Numerical Simulations of Liquefaction and Lateral Spreading. Springer, Cham. https://doi.org/10.1007/978-3-030-22818-7_34 (2020).
3. JICA.: Brief explanation of ‘‘Nalodo” assessment and mitigation, presentation material in National Workshop on Joint Research, Assessment and Mitigation of Liquefaction Hazards (Lesson learned from the 2018 Palu earthquake) (2019).
4. Kiyota, T., Furuichi, H., Hidayat, R., Tada, N., Nawir, H.: Overview of long-distance flow-slide caused by the 2018 Sulawesi earthquake, Indonesia. Soils Found. 60 (3), 722–735 (2020).
5. Kokusho, T. Formation of water film in liquefied sand and its effect on lateral spread. J. Geotech. Geoenviron. Eng. ASCE 125 (10), 817–826 (1999).
6. Kokusho, T.: Current state of research on flow failure considering void redistribution in liquefied deposits. Soil Dyn. Earthq. Eng. 23 (7), 585–603 (2003).
7. Kokusho, T.: Liquefaction Research by Laboratory Tests versus In Situ Behavior. In: Proc. 6th International Conference on Earthquake Geotechnical Engineering, Christchurch, New Zealand, pp. 786–819 (2015)
8. Malvick, E.J., Kutter, B.L., Boulanger, R.W., Kulasingam, R.: Shear localization due to liquefaction-induced void redistribution in a layered infinite slope. J. Geotech. Geoenviron. 132 (10), 1293–1303 (2003).
9. Mason, H.B., Gallant, A.P., Hutabarat, D., Montgomery, J., Reed, N.,Wartman, J., Irsyam, M., Prakoso, W., Djarwadi, D., Harnanto, D., Alatas, I., Rahardjo, P., Simatupang, P., Kawanda, A., Hanifa, R.: The 28 September 2018 M7.5 Palu-Donggala, Indonesia Earthquake: Version 1.0. Geotechnical Extreme Events Reconnaissance Association Report GEER-061, doi:10.18118/G63376 (2019).
10. Montgometry, J., Boulanger, R.W.: Influence of Stratigraphic Interfaces on Residual Strength of Liquefied Soil. 34th Annual United States Society on Dams Conference, San Francisco, CA, 101-111 (2014).
11. Okamura, M., Ono, K., Arsyad, A., Minaka, U.S., Nurdin, S.: Large-scale flowslide in Sibalaya caused by the 2018 Sulawesi Earthquake. Soils Found. 59 (5), 1148–1159 (2019).
12. Sahadewa, A., Irsyam, M., Hanifa, R., Mikhail, R., Pamumpuni, A., Nazir, R., et al.: “Overview of the 2018 Palu Earthquake,” in Proceedings of the 7th International Conference on Earthquake Geotechnical Engineering, Rome, 857–869 (2019).
13. Seed RB, Cetin KO, Moss RES, Kammerer AM, Wu J, Pestana JM, Riemer MF, Sancio RB, Bray JD, Kayen RE, Faris A: Recent advances in soil liquefaction engineering: a unified and consistent framework EERC-2003–06. Earthquake Engineering Research Institute, Berkeley (2003).
14. Sento, N., Kazama, M., Uzuoka, R., Ohmura, H., Ishimaru, M.: Possibility of postliquefaction flow failure due to seepage. J. Geotech. Geoenviron. Eng. 130 (7), 707–716 (2004).